Structure Elucidation of Amide Bonds with Dipolar Chemical Shift NMR Spectroscopy

G. Buntkowsky,* I. Sack, H. H. Limbach, B. Kling, and J. Fuhrhop

Institut für Organische Chemie der Freien Universität Berlin, Takustrasse 3, D-14195 Berlin, Germany

Received: June 10, 1997; In Final Form: October 16, 1997[⊗]

The structure of the amide bonds of gluconamide has been elucidated and compared to acetanilide by the combined application of ^{13}C and ^{15}N double- and triple-resonance solid-state NMR spectroscopy. The length of the amide bond has been determined from the dipolar spectrum using a SEDOR type experiment, and the orientation of the principal axis systems of both the ^{13}C and ^{15}N chemical shift tensors have been determined by employing dipolar chemical shift NMR spectroscopy in conjunction with CSA spectroscopy. The groups exhibit for amide bonds typical approximately 120° bond angles between −CO, −CN, −CR, and −NC, −NH, −NR. Comparing the structure of the gluconamide with the corresponding structure of the acetanilide, two major differences are visible: the orientations of the CSA tensors in the amide plane with respect to the CN-bond direction are different (12° for the ^{13}C tensor and 10° for the ^{15}N tensor), and the directions of least shielding and intermediate shielding are interchanged in the gluconamide as compared to the acetanilide. Since the chemical shielding tensors of the ^{15}N are strongly influenced by hydrogen bonding, these different orientations are an indication of the different hydrogen bond structure of the gluconamide as compared to the acetanilide.

1. Introduction

In recent years ^{13}C and ^{15}N solid-state NMR spectroscopies have become important tools for the structure elucidation of small peptides and proteins.[1] On one hand, the chemical shift interaction is a sensitive probe of structural features such as the primary and secondary structure of the molecule; however, for the interpretation of the corresponding CSA tensors one usually has to employ ab initio calculations of the molecular groups under investigation. Due to the importance of the amide bond as the structure-determining part of the peptide and thus the proteins, these tensors have been investigated in numerous studies of amide and peptide bonds. Magnetic dipolar interactions give direct geometrical information about intra- and intermolecular distances; therefore, this type of interaction has been used in various studies of bond length or intramolecular distances. Due to the axial symmetry of the interaction most information about the relative orientation of the coupled nuclei is not accessible. It is advantageous to apply a combined analysis of chemical shielding anisotropy and dipolar interaction. This approach allows for an orientation of the dipolar vector in the frame of the chemical shielding interaction. Recent studies of ^{13}C-CSA and ^{15}N-CSA tensors and $^{13}C-^{15}N$ dipolar interaction using various solid-state NMR techniques[1] demonstrated the usefulness of this approach. The prime result of all these studies showed the principal components of the CSA tensors of the amide carbon and nitrogen in the various polypeptides investigated to be very similar.[2] The chemical shielding interaction is a local interaction that depends mostly on the molecular and electronic structure close to the nuclei of interest. It was found that for the ^{13}C-CSA tensor the most shielded direction σ_{33} is perpendicular to the NCO plane and the intermediate component σ_{22} is approximately along the −CO bond. For the ^{15}N-CSA the most shielded component points approximately into the direction of the $^{13}C-^{15}N$ bond and the intermediate component is perpendicular to the amide plane.

In the present study ^{13}C and ^{15}N solid state NMR spectroscopies are used for comparing the structure of two different amides, namely, acetanilide (which has been recently studied[1a]) as a reference substance for the NMR structure of amide bonds and *N*-1-octyl-D-gluconamide. The latter compound assembles in bulk water to form micellar fibers in the form of extended quadruple helixes. Such H-bonded fibers have been isolated in the solid state. The molecular conformation of the gluconamide headgroup region has been elucidated by solid-state ^{13}C CP-MAS − NMR spectroscopy[3] and comparisons made with crystal structures of the second, crystalline modification of the *N*-1-octyl-D-gluconamide. It has been found that the linear arrangement of the *N*-1-octyl-D-gluconamide in the crystal (all-trans) is disturbed at C-2. The amide bond conformation was assumed to be trans in all cases, and chemical shift differences of the carboxamide carbon were related to different hydrogen bond lengths. Supporting evidence came from crystal structure and ^{13}C NMR solid-state spectra of the crystals.

In a first step the ^{15}N and ^{13}C dipolar interaction was determined by a variant of the SEDOR[4] experiment. Then the static powder spectra of the ^{15}N and ^{13}C nuclei were measured, and their CSA tensors and the orientation of the dipolar tensors in these CSA frames were determined. The ^{15}N and ^{13}C CSA tensors of the two amides were correlated by dipolar-chemical shift NMR spectroscopy,[1a,h,i] allowing one to determine the relative orientation of the two CSA tensors. Due to the axial symmetry of the dipolar interaction, the two tensors can be rotated along the dipolar axis and there exists a cylindrical ambiguity for the relative orientation.[1a] The usual approach to resolve this ambiguity is the application of symmetry arguments, comparing the system to related systems or ab initio calculations. However one has to be careful in the application of these second-hand arguments.

The rest of the article is organized as follows. After a brief introduction into the theoretical background necessary for understanding how the CSA tensors are correlated with respect to each other, a short description of our experimental setup, sample synthesis, and preparation is given. Then the experimental results are presented and discussed and finally summarized.

* Corresponding author.

[⊗] Abstract published in *Advance ACS Abstracts,* December 1, 1997.

S1089-5647(97)01904-4 CCC: $14.00

2. Theory

As has been well-known for a long time, the anisotropic interactions in solid-state NMR can be described by second rank tensors, i.e., real symmetric 3*3 matrixes.[5] For $I = {}^1/_2$ nuclei and nonconducting organic solids, there are the chemical shielding tensor $\vec{\vec{\sigma}}$, the dipolar interaction tensor $\vec{\vec{D}}$, and the *J*-coupling (which, however, can be neglected in our systems), but no quadrupolar tensor interaction. Thus for a heteronuclear two spin system *I*, *S* the Hamiltonian $\hat{H}$ can be written as:

$$\hat{H} = \gamma_I \vec{B}(1 - \vec{\vec{\sigma}}_I)\hat{I} + \gamma_s \vec{B}(1 - \vec{\vec{\sigma}}_s)\hat{S} + \hat{I}\vec{\vec{D}}\hat{S} \qquad (1)$$

The matrix elements of the dipolar interaction tensor are given as[5d]

$$\vec{\vec{D}}_{mn} = -\frac{\mu_0}{4\pi}\hbar\gamma_I\gamma_S\frac{3(\vec{e}_m\cdot\vec{r}/r)(\vec{e}_n\cdot\vec{r}/r) - \vec{e}_m\cdot\vec{e}_n}{(r)^3} \qquad m, n = x, y, z \quad (2)$$

In high magnetic field only the secular part of the interaction is effective. If B_0 is pointing in the *z*-direction one obtains

$$\hat{H} = \gamma_I B_0(1 - \sigma_{Izz})\hat{I}_z + \gamma_S B_0(1 - \sigma_{Szz})\hat{S}_z + \hat{I}_z D_{zz}\hat{S}_z \qquad (3)$$

All terms in this Hamiltonian commute, and it is diagonal with the following eigenvalues

$$E_1 = +\frac{1}{2}\gamma_I B_0(1 - \sigma_{Izz}) + \frac{1}{2}\gamma_S B_0(1 - \sigma_{Szz}) + \frac{1}{4}D_{zz} \qquad (4)$$

$$E_2 = +\frac{1}{2}\gamma_I B_0(1 - \sigma_{Izz}) - \frac{1}{2}\gamma_S B_0(1 - \sigma_{Szz}) - \frac{1}{4}D_{zz}$$

$$E_3 = -\frac{1}{2}\gamma_I B_0(1 - \sigma_{Izz}) + \frac{1}{2}\gamma_S B_0(1 - \sigma_{Szz}) - \frac{1}{4}D_{zz}$$

$$E_4 = -\frac{1}{2}\gamma_I B_0(1 - \sigma_{Izz}) - \frac{1}{2}\gamma_S B_0(1 - \sigma_{Szz}) + \frac{1}{4}D_{zz}$$

The allowed transitions are (1−2, 3−4) for spin *S* and (1−3, 2−4) for spin *I* with the corresponding transition frequencies

$$\upsilon^S_{(12,34)} = \gamma_S B_0(1 - \sigma_{Szz}) \pm \frac{1}{2}D_{zz} \qquad (5)$$

$$\upsilon^I_{(13,24)} = \gamma_I B_0(1 - \sigma_{Izz}) \pm \frac{1}{2}D_{zz}$$

The tensors $\vec{\vec{D}}$ and $\vec{\vec{\sigma}}$ can be expressed from their diagonal representation in their principal axis system via a rotation $R(\alpha\beta\gamma)$, which can be parametrized using the Euler angles $(\alpha\beta\gamma)$. In general the CSA and the dipolar interaction tensor will have different principal axis systems; thus, for each tensor a separate set of Euler angles is necessary for the transformation.

$$\vec{\vec{D}} = R(\alpha^D\beta^D\gamma^D)\vec{\vec{D}}_{PAS}R(\alpha^D\beta^D\gamma^D)^{-1} = R_D\vec{\vec{D}}_{PAS}R_D{}^{-1} \qquad (6)$$

$$\vec{\vec{\sigma}} = R(\alpha^C\beta^C\gamma^C)\vec{\vec{\sigma}}_{PAS}R(\alpha^C\beta^C\gamma^C)^{-1} = R_C\vec{\vec{\sigma}}_{PAS}R_C{}^{-1}$$

However, it is always possible to first transform the dipolar interaction tensor from its principal frame into the frame of the CSA tensor (D_{CSA}) by a rotation R_{CD} and then do a common transformation into the lab frame:

$$\vec{\vec{D}} = R_C R_{CD}\vec{\vec{D}}_{PAS}R_{CD}{}^{-1}R_C{}^{-1} = R_C\vec{\vec{D}}_{CSA}R_C{}^{-1} \qquad (7)$$

The dipolar tensor in the CSA frame $\vec{\vec{D}}_{CSA}$ and the CSA tensor $\vec{\vec{\sigma}}$ can then be combined to effective shielding tensors $\vec{\vec{\Sigma}}_{PAS}{}^{\pm}$ in the PAS frame of $\vec{\vec{\sigma}}$, which in general are no longer diagonal:

$$\vec{\vec{\Sigma}}_{PAS}{}^{\pm} = \vec{\vec{\sigma}}_{PAS} \mp \vec{\vec{D}}_{CSA} = \vec{\vec{\sigma}}_{PAS} \mp R_{CD}\vec{\vec{D}}_{PAS}R_{CD}{}^{-1} \qquad (8)$$

Transforming these effective interaction tensors into the lab frame, the equations for the transition frequencies can be rewritten as

$$\upsilon^S_{(12,34)} = \gamma_S B_0(1 - \vec{\vec{\Sigma}}^{S\pm}{}_{zz}) \qquad (9)$$

$$\upsilon^I_{(13,24)} = \gamma_I B_0(1 - \vec{\vec{\Sigma}}^{I\pm}{}_{zz})$$

While in single crystals only two lines for each spin are observable, in a powder the average over all possible orientations has to be taken into account. Due to the axial symmetry of the magnetic field, it is sufficient to integrate over two angles (ϑ,ϕ) only. Thus, assuming that T_2 is the transversal relaxation time, which for simplicity is assumed to be orientational independent, the spectra can be calculated as

$$S(\nu) = \int_0^{\pi} d\vartheta \sin(\vartheta) \int_0^{2\pi} d\varphi \left(\frac{T_2^S}{1 + 4\pi^2(T_2^S(\nu - \nu_{12}(\vartheta\varphi)))^2} + \frac{T_2^S}{1 + 4\pi^2(T_2^S(\nu - \nu_{34}(\vartheta\varphi)))^2} \right) \qquad (10)$$

$$I(\nu) = \int_0^{\pi} d\vartheta \sin(\vartheta) \int_0^{2\pi} d\varphi \left(\frac{T_2^I}{1 + 4\pi^2(T_2^I(\nu - \nu_{13}(\vartheta\varphi)))^2} + \frac{T_2^I}{1 + 4\pi^2(T_2^I(\nu - \nu_{24}(\vartheta\varphi)))^2} \right)$$

The result is for each spin a superposition of two powder patterns, where the singular values of the two patterns are determined by the principal values of the tensors $\vec{\vec{\Sigma}}^{S\pm}$ or $\vec{\vec{\Sigma}}^{I\pm}$. As the effective interaction tensors $\vec{\vec{\Sigma}}^{S\pm}$ and $\vec{\vec{\Sigma}}^{I\pm}$ depend, via the rotations $R^S{}_{CD}$ and $R^I{}_{CD}$, on the mutual orientations of the chemical shift and dipolar interaction tensor, simulating the *I* and *S* spin spectra (using eq 10), it is possible to orient the dipolar vector in the coordinate frame of each shielding interaction. Thus one obtains information about the mutual orientation of the two shielding tensors. By successive pairwise labeling of molecules (or more generally aggregates, since the dipolar interaction does not depend on the existence of a direct or indirect chemical bond between the interacting nuclei), it is possible to map the complete geometrical structure of the aggregate.

If second-order quadrupolar interaction is neglected, the extension to nuclei with $I > {}^1/_2$ is straightforward. Instead of two effective tensors $\vec{\vec{\Sigma}}^{S\pm}$ there are now $(2I + 1)$ tensors $\vec{\vec{\Sigma}}^{Sm}$, where *m* varies from $-I$ to *I*. However, there exists a particular problem for nuclei with integer spin *I* (for example ^{2}H), as the transitions with $m = 0$ occur at the same resonance frequency as the transitions of *S* nuclei bound to a proton. Thus in these cases, to correct for imperfect isotope labeling, it is useful to introduce a labeling factor to the $m = 0$ transition. In the case of isotopes with half-integer spin *I*, the spectra of the unlabeled system will be different from all the subspectra and thus no such problems exist.

3. Materials and Methods

3.1. The Spectrometer. A scheme of our experimental setup is shown in Figure 1. All experiments were performed

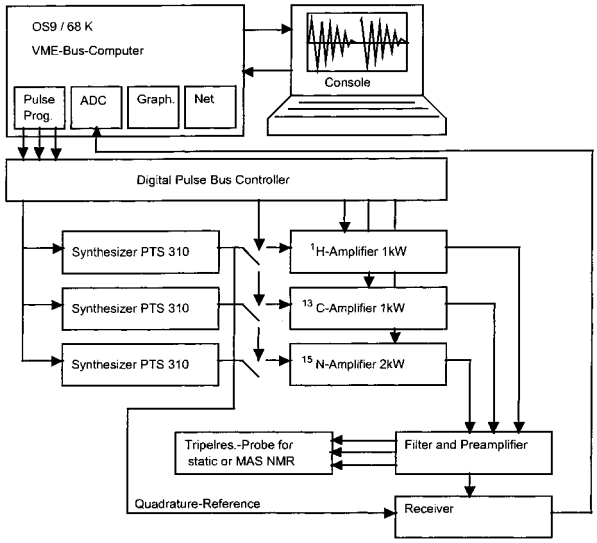

Figure 1. Scheme of experimental setup.

at a field of 6.98 T, corresponding to a proton resonance frequency of 297.8 MHz on a standard Oxford wide bore magnet (89 mm) equipped with a room temperature shim unit. We used a home-built three channel NMR spectrometer, with all three channels are controlled by a pulse programmer with 100 ns resolution, 32-bit binary output, and 32k maximum pulse program length. Each channel consists of a digital-controlled (DDS) synthesizer for generating the NMR frequencies. The necessary phases are generated by directly switching the phase of the digitally controlled synthesizers.[6] After the synthesizer, the actual pulses were generated with fast RF-switches (10 ns rise time) and fed into the power amplifiers. For the proton channel a Creative Electronics 1 kW class C amplifier was used. For the ^{13}C-channel a 1 kW class AB and for the ^{15}N-channel a 2 kW class AB amplifier, both from AMT, were employed. All amplifiers are equipped with an RF-blanking for suppressing the noise during data aquisition. All experiments were performed using a commercial Doty triple-resonance NMR probe operating at room temperature. To improve the mutual RF-isolation of the three channels commercial band-pass filters (Texscan) in conjunction with home-built notch filters were employed. The RF of the observed channel was fed through a crossed diode duplexer, connected to the detection preamplifier and through the filters into the probe. The other two channels were fed directly through the filters into the probe. Typical 90° pulse width was 6.5 μs for all three channels, corresponding to a B_1-field in frequency units of $\nu_1 = 38$ kHz. This was sufficient to remove ^{1}H-X dipolar line broadening. Repetition time of the experiments was 10 s for the gluconamide and 30 s for the acetanilide. To avoid dead time problems caused by the rather high Q of the probe, we measured all spectra using a fully phase cycled spin−echo technique. The spectra were measured by first cross-polarizing the observed nucleus from the protons and then recording the spin−echo signal under proton decoupling. Typical echo delay was 300 μs. For the ^{15}N−^{13}C samples the labeling was better then 99%; therefore, no labeling factor had to be included. However for the simulation of the ^{15}N−^{2}H spectra, we had to include a labeling factor to account for imperfect deuteration of the −NH group. The referencing of the tensor values was accomplished by determining the isotropic chemical shift value from the ^{13}C and ^{15}N CP-MAS spectra, measured at 7 kHz spinning speed, and adjusting the trace of the fitted tensors to this value.

The ^{15}N−^{13}C dipolar coupling constant of acetanilide was measured independently by employing a variant of the SEDOR

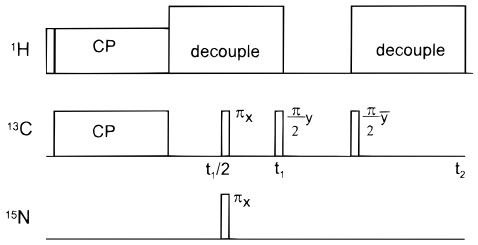

Figure 2. SEDOR type pulse sequence for measuring heteronuclear dipolar couplings. The simultaneous irradiation of the π-pulses at $t_1/2$ in the ^{13}C and ^{15}N channels refocuses the evolution under the chemical shift Hamiltonian at time t_1. The partial echo, which is modulated by the dipolar interaction, is converted into z-magnetization by a $(\pi/2)y$-pulse. After dephasing of remaining transverse magnetization the z-magnetization is read out with a $(\pi/2)/\bar{y}$-pulse. Fourier transformation with respect to t_1 gives the dipolar spectrum.

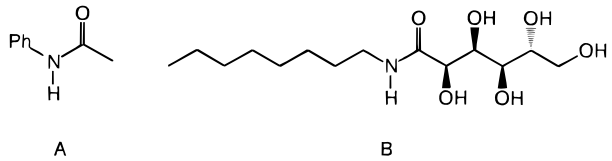

Figure 3. Formula of (A) acetanilide and (B) gluconamide.

experiment,[4,5a] which is a variation of the 2D-experiment described for measuring homonuclear dipolar couplings.[7] The basic sequence is shown in Figure 2. After cross-polarization and delay t_1, a 180° pulse is applied simultaneously to the ^{15}N and ^{13}C channel. As a result of these pulses after the time $2t_1$ a partial echo is formed, where the chemical shielding interaction is selectively refocused, and the spins evolve only under the ^{13}C−^{15}N dipolar interaction. By applying a 90° pulse to the ^{13}C, this echo is stored as z-magnetization, and after a dephasing delay without proton decoupling of 10 ms, all remaining transversal coherences are destroyed. The stored ^{13}C echo signal is then read by either a 90° pulse for recording a 2D spectra or by a CPMG sequence for recording the dipolar FID directly.

3.2. Samples and Preparation. Acetanilide (Figure 3a) was used as a standard reference for the experiments with the various isotopic configurations. Acetanilide has several advantageous features: it is rather easy to perform the selective isotope labeling, and its crystal structure and NMR parameters are known. The synthesis of isotopically labeled acetanilide was performed in the standard way[8a] by adding a solution of acetyl chloride (either unlabeled or 99% ^{13}C(CO) labeled from Chemotrade, Leipzig, Germany) in chloroform to aniline (either unlabeled or 99% ^{15}N labeled, also from Chemotrade, Leipzig, Germany) solved in chloroform and stirred in an ice bath. The addition was completed at a higher temperature of about 50 °C. The solution was stirred for 1 h, and the excess solvent removed to yield crystals of acetanilide that were recrystallized in water.

The synthesis of the selectively isotope labeled gluconamide (Figure 3b) samples is described in detail elsewhere[8b] and will only be briefly summarized here. For the synthesis of the ^{15}N single labeled *N*-1-octyl-D-gluconamide 99% [^{15}N]ammonia produced from ammonium chloride was employed. In a first step [^{15}N]ammonia was condensed into a solution of octanoyl chloride in diethyl ether at −40 °C, which lead to the spontaneous formation of [^{15}N]octylamide, which precipitated from the solution. After filtering and recrystallization from water, pure [^{15}N]octylamide was obtained. In a second step, by reduction with $LiAlH_4$, [^{15}N]octylamin was obtained. In the last step by aminolysis with D-gluconic acid-δ-lacton the *N*-1-octyl-D-gluconamide was obtained. The ^{15}N−^{13}C double labeled compound was synthesized by employing ^{13}C-labeled

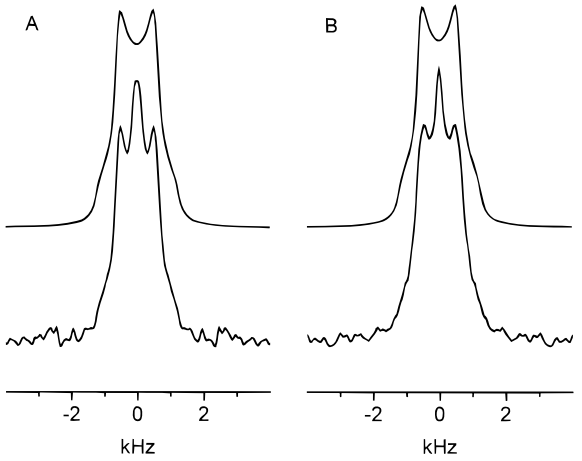

Figure 4. Dipolar ^{13}C NMR spectra of (A) $^{13}C-^{15}N$ doubly labeled acetanilide and (B) $^{13}C-^{15}N$ doubly labeled gluconamide after the SEDOR sequence (Figure 2). Experimental (lower curves) and simulated (upper curves) spectrum. The intensity in the center of the experimental spectra stems from bulk ^{13}C nuclei, which have no ^{15}N partner.

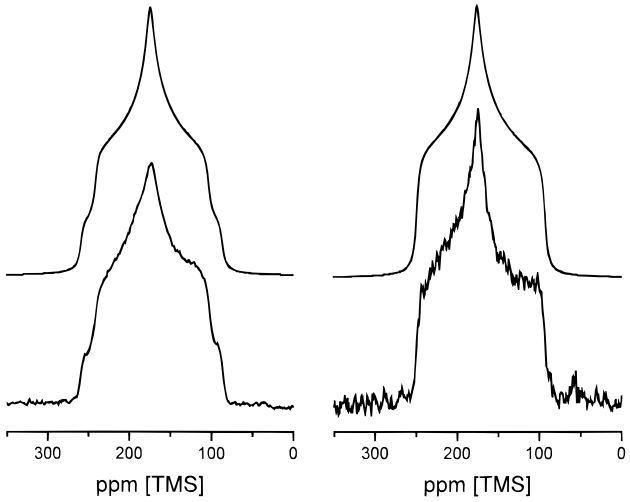

Figure 5. ^{13}C NMR spectrum of $^{13}C-^{15}N$ doubly labeled acetanilide. Experimental (lower curves) and simulated spectra (upper curves). (Left panel) The full dipolar CSA spectrum (i.e., without ^{15}N decoupling). (Right panel) Only the CSA is visible; i.e., the dipolar interaction is suppressed by ^{15}N decoupling.

D-gluconic acid-δ-lacton, synthesized from 98.5% ^{13}C-labeled D-glucose (Sigma). The deuterated samples were produced by boiling 150 mg ^{15}N-labeled *N*-1-octyl-D-gluconamide in 3 mL of 99% D_2O. The material was placed into a standard 5 mm high-speed Doty rotor with KELF caps, which sealed the sample sufficiently tight to prevent structural modifications or rehydrogenation of the deuterated sample by moist air.

3.3. Data Evaluation. The echo spectra after phase correction were simulated using eq 10. Instead of numerically performing the powder integration of eq 10, the analytical expression of the powder pattern in terms of elliptic integrals[5c] was used to calculate the line shape for zero width from the eigenvalues of the effective interaction tensors $\vec{\Sigma}^{S\pm}$. This line was then numerically convoluted with a Lorentzian by Fourier transforming into the time domain, multiplying with a decaying exponential function, and transforming back into the frequency domain to give the spectra of eq 10.

4. Results and Discussion

4.1. Experimental Results. In the following the experimental results obtained from the ^{13}C and ^{15}N spectra, that are summarized in Tables 1−3 will be presented. Figure 4a shows the experimental dipolar ^{13}C NMR spectrum of the $^{13}C-^{15}N$ doubly labeled acetanilide after the SEDOR sequence described above.

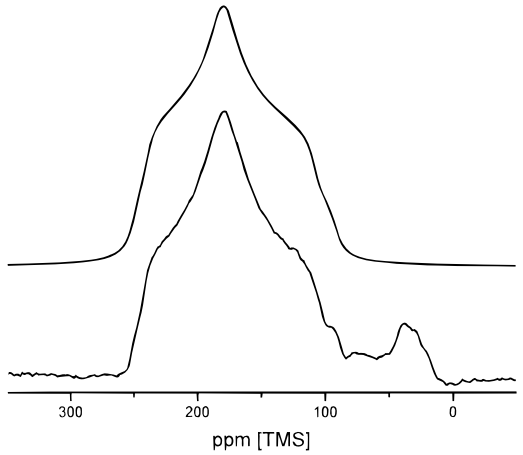

Figure 6. ^{13}C dipolar CSA NMR spectra of $^{13}C-^{15}N$ doubly labeled gluconamide. Experimental (lower curves) and simulated spectra (upper curves). In the range between 100 and 0 ppm there is additional spectral intensity from natural abundance bulk ^{13}C.

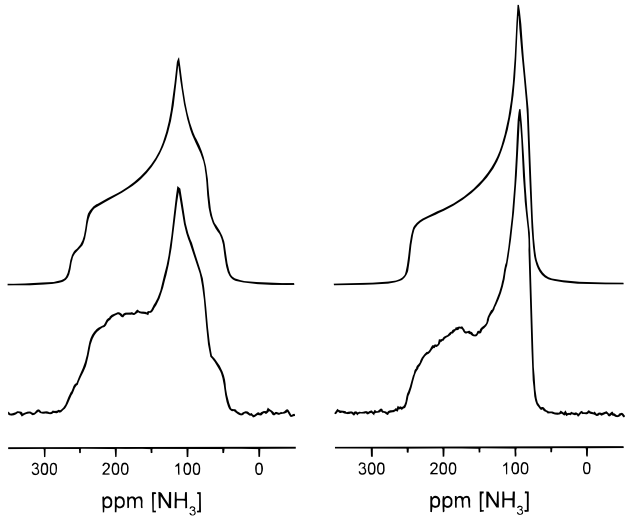

Figure 7. ^{15}N dipolar CSA NMR spectra of $^{13}C-^{15}N$ doubly labeled acetanilide. Experimental (lower curves) and simulated spectra (upper curves). (Left panel) The full dipolar CSA spectrum (i.e., without ^{13}C decoupling). (Right panel) Only the CSA is visible, i.e., the dipolar interaction is suppressed by ^{13}C decoupling.

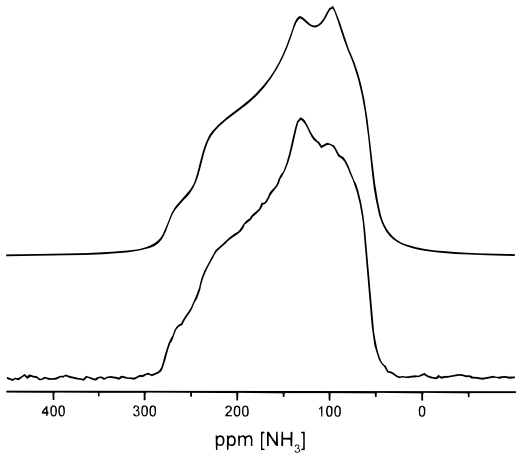

Figure 8. ^{15}N dipolar CSA NMR spectrum of $^{13}C-^{15}N$ doubly labeled gluconamide. Experimental (lower curves) and simulated spectra (upper curves).

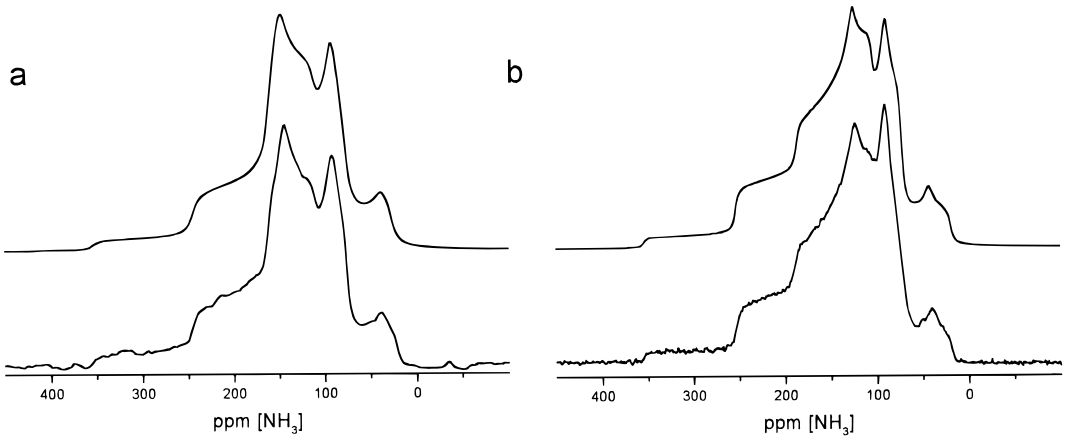

Figure 9. ^{15}N dipolar CSA NMR spectra of ^{2}H−^{15}N doubly labeled acetanilide (A, left panel) and of ^{2}H−^{15}N doubly labeled gluconamide (B, right panel). Experimental (lower curves) and simulated spectra (upper curves).

The central part of the experimental spectrum has some additional Lorentzian contribution, which can be attributed mainly to bulk ^{13}C atoms. The outer parts of the spectrum exhibit the typical Pake pattern of a heteronuclear spin pair. Therefore, for the simulation of the experiment, the central part of the spectrum was ignored and the theoretical dipolar powder pattern was adjusted to the outer wings of the spectrum. This gave a coupling constant of 1220 ± 30 Hz, which corresponds to a CN distance of 1.35 ± 0.01 Å, which is in very good agreement with the value of 1230 ± 40 Hz, given by ref 1a as well as with the value of 1220 Hz calculated from the distance obtained by crystal structure (1.354 Å).[9] Figure 4B shows the experimental dipolar ^{13}C NMR spectrum of the ^{13}C−^{15}N doubly labeled gluconamide after the same SEDOR sequence as above, which gave the same dipolar coupling of 1220 ± 30 Hz (1.35 ± 0.01 Å).

Figure 5 compares the ^{13}C NMR spectra of the ^{13}C−^{15}N doubly labeled acetanilide. By ^{15}N decoupling, the dipolar interaction to the ^{15}N nucleus is suppressed (right side of the figure), and thus the pure ^{13}C−CSA spectrum is measured. The left figure, which is recorded without ^{15}N decoupling, depicts the full dipolar CSA spectrum. From the pure CSA spectrum the principal values of the CSA tensor were obtained. These were used in conjunction with the dipolar coupling constant obtained from the SEDOR experiment (Figure 4A) for simulating the dipolar CSA spectra by fitting the orientation of the dipolar vector in the frame of the CSA tensor.

Figure 6 shows the corresponding ^{13}C NMR spectrum of the gel modification of the ^{13}C−^{15}N doubly labeled gluconamide. The CSA parameter obtained from the spectrum with ^{15}N decoupling (not shown) was used in conjunction with the dipolar coupling from the SEDOR experiment (Figure 4B) to perform the simulation of the full dipolar CSA spectrum from which the orientation of the dipolar vector in the CSA frame was obtained. In the same way, the ^{15}N spectra of the ^{15}N−^{13}C-labeled acetanilide and gluconamide samples were recorded and evaluated. The resulting spectra and simulations are shown in Figure 7 (acetanilide) and Figure 8 (gluconamide). Figure 9 displays the ^{15}N spectra of the ^{15}N−^{2}H-labeled acetanilide and gluconamide samples. While the deuteration of the acetanilide was better than 99% for the gluconamide, we had to adapt an isotope labeling factor of 80 ± 5% in the simulation to account for the partial deuteration of the sample. The spectra were simulated using the CSA parameter from the ^{15}N−^{13}C-labeled samples by adjusting the strength and orientation of the dipolar coupling vector in the CSA frame.

4.2. Discussion. In the following the notation of Lumsden[1a] is used; i.e., the principal values of the CSA interaction are termed δ_{11} (least shielded), δ_{22} (intermediate), and δ_{33} (most shielded). The parameters of the various CSA NMR tensors are summarized in Tables 1−3. To avoid asymmetry parameters of $\eta > 1$, we defined $\eta = (\delta_{22} - \delta_{33})/(\delta_{11} - \delta_{iso})$ instead of the usual $\eta = (\delta_{22} - \delta_{11})/(\delta_{33} - \delta_{iso})$ for the ^{15}N tensors. In the notation of bond vectors the first nuclei always refers to the observed nuclei (i.e. −CN vector, ^{13}C observed; −NC vector, ^{15}N observed).

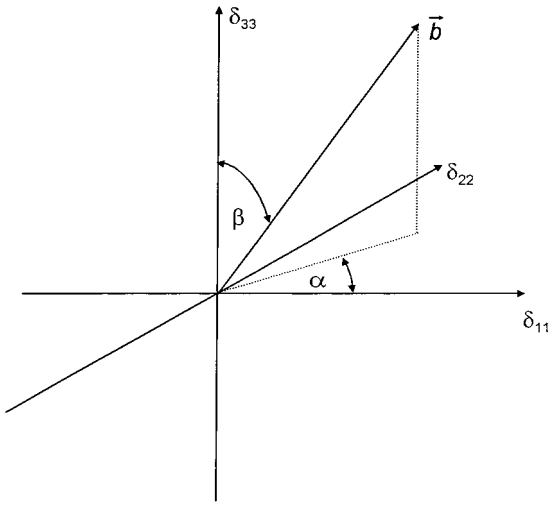

Figure 10. Definitions of the polar angles α and β that characterize the direction of the dipolar interaction in the coordinate frame of the CSA interaction.

4.2.1. Orientation of the Acetanilide ^{13}C CSA Tensors in the Molecular Frame. For the orientation of the acetanilide ^{13}C CSA tensors (Table 1) in the molecular frame, we used the constraint that, because of the planar symmetry of the amide group, one of the principal axis of the tensor is perpendicular to the amide plane and that the −CN bond direction, which is also the direction of the dipolar vector, lies in the amide plane. The δ_{33}-axis is the only axis perpendicular to the ^{13}C−^{15}N dipolar vector. It follows that the δ_{33}-axis is the axis perpendicular to the amide plane and the −CN and −CO bonds are in the (δ_{11},δ_{22}) plane.

Since the sign of the angle α_N is not known, there are two possible orientations of the −CN bond in the (δ_{11},δ_{22}) plane. These are shown as vectors CN_A and CN_B in Figure 11a, which shows a sketch of the ^{13}C geometry in the (δ_{11},δ_{22}) frame (the carbonyl carbon is in the center of the coordinate system). In configuration A the −CN vector CN_A is rotated with an angle $\alpha_{AN} \approx +33°$ with respect to the δ_{11} axis, and in configuration B the −CN vector CN_B is rotated with an angle $\alpha_{BN} \approx -33°$

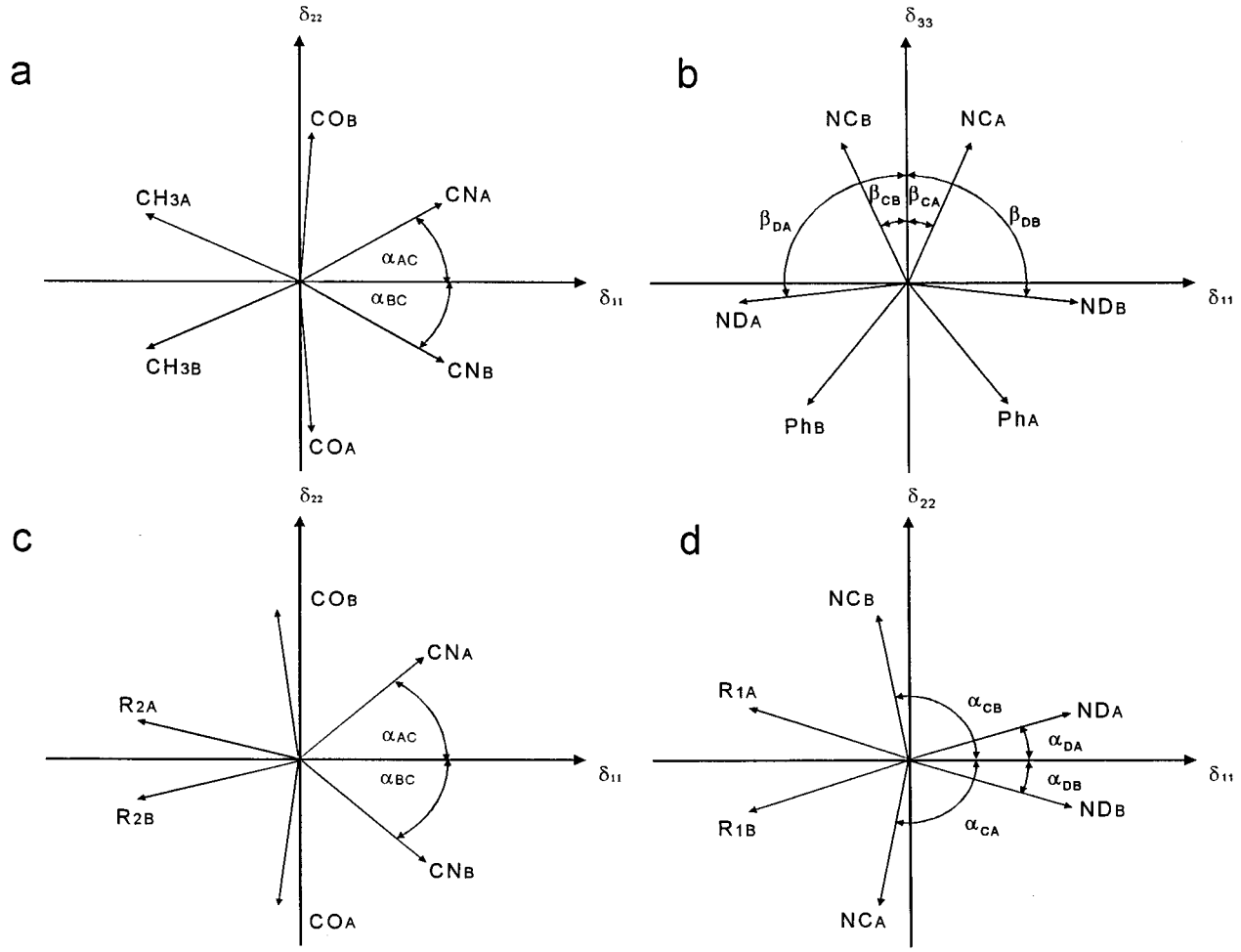

Figure 11. Orientation of the bond directions in the (a) ^{13}C and (b) ^{15}N CSA frame of the acetanilide and in the (c) ^{13}C and (d) ^{15}N CSA frame of the gluconamide. From these orientations the molecular geometry of the group can be constructed.

with respect to the δ_{11} axis. Because of the sp^2-hybridization of the carbonyl C, the bond angle between the −CN and the −CO bond is approximately 120°, and there are two possible orientations for the −CO bond. For configuration A the CO_A vector could point either at an angle of ≈153° or at an angle of ≈273° with respect to the δ_{11}-axis, while for configuration B the CO_B vector points either at an angle of ≈87° or at an angle of ≈207° with respect to the δ_{11}-axis. By NMR alone it is not possible to decide between these two configurations. It has been shown in ref 1a that this problem can be solved by employing additional data. Molecular orbital calculations[10] have shown that the most shielded component is perpendicular to the carbonyl plane and the least shielded component is perpendicular to the carbonyl bond and in the carbonyl plane. It follows that the intermediate component δ_{22} is close to the carbonyl bond. This is only fulfilled for the bond vectors CO_B and CO_A, belonging to the configurations A or B respectively, which also determines the direction of the bond to the $-CH_3$ group, shown as CH_{3A} and CH_{3B} respectively. The resulting two configurations A and B are symmetry related via a 180° rotation around the δ_{11}-axis.

4.2.2. Orientation of the Acetanilide ^{15}N CSA Tensors in the Molecular Frame. For the orientation of the ^{15}N CSA tensors in the molecular frame two orientation constraints are available: The direction of the −NC bond in the ^{15}N CSA frame from the ^{15}N spectrum of the $^{15}N-^{13}C$-labeled compound and the direction of the −ND bond in the ^{15}N CSA frame from the ^{15}N spectrum of the deuterated compound. However, this advantage is reduced by the nearly axial symmetry of the ^{15}N CSA tensor. Therefore, we used the constraint that, because of the planar symmetry of the amide group, one of the principal axis of the tensor is perpendicular to the amide plane and that the −NC bond direction, which is also the direction of the $^{15}N-^{13}C$ dipolar vector, lies in the amide plane. Using the angles from Table 2 and Table 3 it follows that the (δ_{11},δ_{33}) plane is the amide plane and that the δ_{22} axis is the axis perpendicular to that plane and that the −NC vector as well as the −ND vector are both in the (δ_{11},δ_{33}) plane. The signs of the angles β_D and β_C are not known, and there are two possible orientations for the −ND and the −NC vector in the (δ_{11},δ_{33}) plane. However, it is well-known that the ^{15}N atom in an amide group is in a nearly sp^2-configuration with an angle of approximately 120° between −NC and −ND vector. There are two possible combinations of the −NC and −ND vectors to fulfill this constraint, shown as configurations A and B in Figure 11b. In the first combination A, the vector NC_A is rotated $\beta_{CA} = -22°$ with respect to the δ_{33}-axis and has to be combined with the vector ND_A stemming from the (180°−83°) rotated −ND vector. In the second configuration B, the vector NC_B is rotated $\beta_{CB} = 22°$ with respect to the δ_{33}-axis and has to be combined with the vector ND_B, stemming from the −(180°−83°) rotation with respect to the δ_{33}-axis. The resulting two configurations A and B are symmetry related via a 180° rotation around the δ_{33}-axis.

4.2.3. Orientation of the Gluconamide ^{13}C CSA Tensors in the Molecular Frame. The isotropic chemical shielding of the gluconamide ^{13}C CSA tensor gives the typical value of a carbonyl carbon and the principal values of the gluconamide ^{13}C CSA tensor as well as the $^{13}C-^{15}N$ dipolar interaction

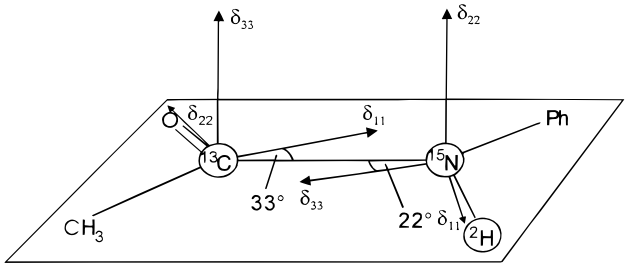

Figure 12. Geometrical structure of the amide group in acetanilide.

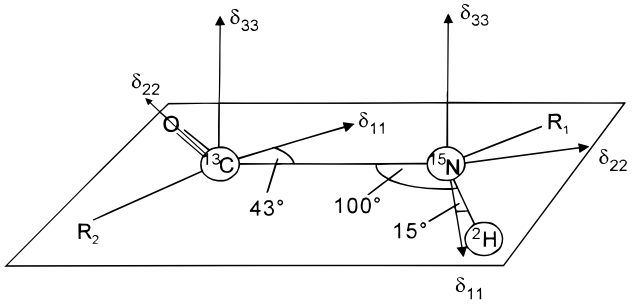

Figure 13. Geometrical structure of the amide group in gluconamide.

strength and direction in the ^{13}C CSA frame are comparable to the values obtained for the acetanilide. Therefore, the same reasoning can be used to orient the ^{13}C CSA tensor with respect to the molecular frame of the amide group, and again two symmetry-related configurations are found, which are shown in Figure 11c. Comparing this figure with Figure 11a, it is evident that for the gluconamide the bond directions in the CSA frame are rotated approximately 12° as compared to the acetanilide. This indicates that there are differences in the electronic structure of the amide groups, and these differences are also reflected in the asymmetry parameter $\eta = 0.80$ and in the intermediate shielding value δ_{22}.

4.2.4. Orientation of the Gluconamide ^{15}N CSA Tensors in the Molecular Frame. The values of the polar angles of the dipolar interaction vectors for the gluconamide exhibit an interesting difference as compared to the values of the acetanilide. For the gluconamide the angle β between the δ_{33} axis and both the −NC (Table 2) and −ND (Table 3) bond direction is 90°. Thus the least shielded component is perpendicular to the amide plane and not the intermediate component δ_{22} of the CSA tensor, and the amide plane is spanned by the (δ_{11},δ_{22}) components of the CSA tensor. The direction of the bonds in the (δ_{11},δ_{22}) plane is determined by the angle α. Following the same arguments as above, there are two different orientations corresponding to ±α, the angle between the bond direction and the δ_{11}-axis. Employing the argument that the angle between the −CN and −ND direction is approximately 120°, it is possible to assign the corresponding bond axes to each other, which are marked as configuration A or B in the Figure 11d. The two configurations are symmetry related via a C_2 rotation around the δ_{11}-axis of the CSA tensor.

4.2.5. Structure of the Amide Group of the Acetanilide. From the previous discussion, the geometrical structure of the amide group can be constructed. Rotational symmetry along the CN bond means it is not possible by NMR alone to decide if the molecule exists in the cis or trans form. This ambiguity can be resolved by employing X-ray data,[9] and these data show that in the solid state the trans configuration is preferred. The resulting structure of the amide group including the directions of the CSA tensors is displayed in Figure 12.

4.2.6. Structure of the Amide Group of the Gluconamide. Once more, due to the rotational symmetry with respect to the CN bond, it is not possible by NMR alone to decide whether the amide group occurs in the cis or trans form. X-ray data of the molecule are only available for the crystalline modification of the gluconamide, where the trans form is preferred, but not for the fibrous form. The question of whether the molecule, in its fibrous form, exists in the cis or trans form can be resolved by employing additional data from ^{13}C-CPMAS NMR and infrared spectroscopy. Such data point to the trans diastomer as the preferential configuration. Figure 13 depicts the resulting structure of the amide group of the gluconamide, including the directions of the CSA tensors.

5. Summary and Conclusion

The ^{13}C and ^{15}N solid-state NMR spectra of acetanilide and gluconamide have been recorded, and the corresponding chemical shift and dipolar interaction tensors have been determined. Our results on the principal values and orientations of the acetanilide ^{13}C tensors corroborates the data presented by Lumsden et al.[1a] From these data the complete geometrical structures of the amide group of the acetanilide and gluconamide were determined. The groups exhibit amide and peptide bonds of typical approximately 120° bond angles between −CO, −CN, −CR, and −NC, −NH, −NR. Comparing the NMR results from the two amide groups, several noteworthy differences are evident. (i) The eigenvalues of the gluconamide ^{13}C tensor exhibit a weaker high field shift (4 ppm) compared to acetanilide. (ii) The orientation of the δ_{11}-axis of the gluconamide ^{13}C tensor is 12° farther away from the CN-bond direction, the CN bond is intersecting the δ_{11},δ_{22} angle (45°) and the anisotropy of the ^{13}C tensor is stronger. (iii) The ^{15}N CSA tensor is shifted to high field and exhibits a stronger anisotropy. (iv) The amide plane is spanned by the (δ_{11},δ_{22}) components of the ^{15}N CSA tensor but not by the (δ_{11},δ_{33}) components.

There are two possible explanations for these differences, which are not necessarily mutually exclusive. They can be due to intramolecular effects, such as different head and tail groups and different conformations of the head and tail groups, or by intermolecular effects such as N−H···O═C intermolecular hydrogen bonding. Differences in the ^{13}C isotropic shift of amide ^{13}CO values have been attributed to different hydrogen-bonding lengths;[3,11] furthermore, it has been found that all three components of a ^{15}N-CS tensor are very sensitive to the geometry of the hydrogen bonding.[2g,1a] In the gluconamide the neighboring carbon atom of the amide group is in an sp^3-configuration, and in the acetanilide the neighboring carbon atom is in an sp^2-configuration, which could account for the difference. However, ^{15}N−^{2}H dipolar NMR experiments have shown[13] that for sp^3-configurations of the neighboring carbon atom the same tensor orientation as in the case of the acetanilide can be found as well. This suggests that the intramolecular

TABLE 1: Parameters from the ^{13}C−^{15}N-Labeled ^{13}C Spectra

^{13}C−^{15}N	δ_{11} (ppm)	δ_{22} (ppm)	δ_{33} (ppm)	δ_{iso} (ppm)	η	α	β	D (Hz)
AA	248(2)	175(1)	90(2)	171	0.90	30(5)	90(3)	1230(40)
AA[b]	247(1)	173(1)	94(1)	171	0.95	33	90	1220
GA[c]	243(1)	183(1)	100(1)	175	0.80	43	90	1220

[a] Acetanilide data from ref 1a. [b] Acetanilide, own results. [c] Gluconamide.

TABLE 2: Parameters from the $^{15}N-^{13}C$ Labeled ^{15}N Spectra

$^{15}N-^{13}C$	δ_{11} (ppm)	δ_{22} (ppm)	δ_{33} (ppm)	δ_{iso} (ppm)	η	α	β	D (Hz)
AA[a]	247(1)	90(1)	77(1)	138	0.12	0(10)	20(3)	1230(40)
AA[b]	245(1)	89(1)	77(1)	137	0.11	0	22.1	1220
GA[c]	239(1)	76(1)	57(1)	124	0.17	100	89	1220

[a] Acetanilide data from ref 1a. [b] Acetanilide, own results. [c] Gluconamide.

TABLE 3: Parameters from the $^{15}N-^{2}H$-Labeled ^{15}N Spectra

$^{15}N-^{2}H$	δ_{11} (ppm)	δ_{22} (ppm)	δ_{33} (ppm)	δ_{iso} (ppm)	η[d]	α	β	D (Hz)
AA[a]	247(1)	90(1)	77(1)	138	0.12	0(3)	83(3)	1690(40)
AA[b]	245(1)	89(1)	77(1)	137	0.11	0	81	1640
GA[c]	239(1)	76(1)	57(1)	124	0.17	15	90	1600

[a] Acetanilide data from ref 1a. [b] Acetanilide, own results. [c] Gluconamide. [d] To remain consistent with the notation of the principal values used by Lumsden,[1a] but avoid values of $\eta > 1$, we defined $\eta = (\delta_{22} - \delta_{33})/(\delta_{11} - \delta_{iso})$ instead of the usual $\eta = (\delta_{22} - \delta_{11})/(\delta_{33} - \delta_{iso})$.

effects are not responsible for the differences in the local electronic structure, which is reflected in the differences in the shielding parameters. The N−H···O═C intermolecular hydrogen bond is the main structural element responsible for the formation of the extended quadruple helixes in the fibrous modification of the gluconamide molecules. Therefore, we conclude that differences in the intermolecular hydrogen bonding are the principal reason for the differences in the tensor orientations. This suggests that to obtain reasonable results from ab initio calculations of amide and peptide bonds, it is important not only to include the local molecular configuration but also to include information about the neighboring molecules.

It has been demonstrated that dipolar chemical shift NMR spectroscopy can give valuable information about the structure of small molecular groups. The possible information gain from this method can be greatly enhanced by combining this form of NMR spectroscopy with additional NMR methods, for example, SEDOR experiments for directly measuring the strength of dipolar couplings or selectively switching on and off heteronuclear dipolar couplings by decoupling of the second X-nuclei and CP-MAS techniques for determining the isotropic shielding values. These additional methods are demanding concerning the necessary experimental setup, because at least a three-channel NMR spectrometer is needed. It has been shown that acetanilide, because of its favorable NMR parameters and simple labeled synthesis, is a convenient standard for setting up these experiments. As an application to a larger molecule, the structure of the amide group of the *N*-1-octyl-D-gluconamide in its fibrous modification has been determined.

Finally the question arises whether these methods permit the study of larger structures, for example, small peptides or oligonucleotides, where several bonds have to be correlated to each other to give the complete geometrical structure of the molecule. For these cases, the absence of the isotropic chemical shift resolution (which would be given, for example, by MAS type experiments) is a strong restriction for the applicability of the method, because it demands pairwise selective isotopic labeling, for example, of the sequence of amino acids, which is very demanding concerning the synthetic expense. Therefore, for these types of systems, it is advantageous to apply MAS techniques combined with dipolar recoupling sequences.[12] However, these experiments provide only very indirect access to the orientational correlation of dipolar interactions, which represent bond directions and chemical shift tensors that represent the local electronic structure. If this information is desired, it is therefore necessary to perform the labeled synthesis and apply the techniques described in this paper.

Acknowledgment. This work was supported by the German Israel Foundation under Grant G.I.F. Research Grant No. I-297.092.05/93.

References and Notes

(1) See, for example: (a) Lumsden, M. D.; Wasylishen, R. E.; Eichele, K.; Schindler, M.; Penner, G. H.; Power, W. P.; Curtis, R. D. *J. Am. Chem. Soc.* **1994**, *116*, 1403. (b) Ando, S.; Ando, I.; Shoji, A.; Ozaki, T.; Tabeta, R.; Saito, H. J. *J. Am. Chem. Soc.* **1985**, *107*, 7848. (c) Ando, S.; Yamanobe, T.; Ando. I.; Shoji, A.; Ozaki, T. *J. Mol. Struct.* **1989**, *192*, 153. (d) Asakawa, N.; Kuroki, S.; Kurosu, H.; Ando, I.; Shoji, A.; Ozaki, T. *J. Am. Chem. Soc.* **1992**, *114*, 3261. (e) Shoji, A.; Ozaki, T.; Fujito, T.; Deguchi, K.; Ando, S.; Ando. I. *Macromolecules* **1989**, *22*, 2860. (f) Shoji, A.; Ozaki, T.; Fujito, T.; Deguchi, K.; Ando, S.; Ando, I. *J. Am. Chem. Soc.* **1992**, *112*, 4693. (g) Kuroki, S.; Asakawa, N.; Ando, S.; Ando, I.; Shoji, A.; Ozaki, T. *J. Mol. Struct.* **1991**, *245*, 69. (g) Shoji, A.; Ando, S.; Kuroki, S.; Ando, I.; Webb, G. A. *Annu. Rep. NMR Spectrosc.* **1993**, *26*, 55. (h) Hoelger, C. G.; Limbach, H. H. *J. Phys. Chem.* **1994**, *98*, 11803. (i) Hoelger, C. G.; Limbach, H. H.; Aguilar-Parrilla, F.; Elguéro, J.; Weintraub, O.; Vega, S. *J. Magn. Reson.* **1996**, *A120*, 46.

(2) (a) Duncan, T. M. *A Compilation of Chemical Shift Anisotropies*; The Farragut Press: Chicago, IL, 1990. (b) Zhengtian Gu; Zambrano, R.; McDermott, A. *J. Am. Chem. Soc.* **1994**, *116*, 6368.

(3) Svenson, S.; Kirste, B.; Fuhrhop, J. H. *J. Am. Chem. Soc.* **1994**, *116*, 11969.

(4) (a) Kaplan D. E.; Hahn E. L. *J. Phys. Radium* **1958**, *19*, 821. (b) Kaplan, D. E.; Hahn, E. L. *Bull. Am. Phys. Soc.* **1957**, *2*, 384. (c) Emshwiller, M.; Hahn, E. L.; Kaplan, D. E. *Phys. Rev. Lett.* **1960**, *118*, 414.

(5) See, for example: (a) Slichter C. P. *Principles of Magnetic Resonance*, 3rd ed.; Springer-Verlag: Berlin, Heidelberg, New York, 1990. (b) Abragam, A. *Principles of Nuclear Magnetism*; Clarendon Press: Oxford, 1961. (c) Mehring, M. *High-Resolution NMR Spectroscopy in Solids*; Springer-Verlag: Berlin, Heidelberg, New York, 1983. (d) Schmidt-Rohr, K.; Spiess, H. W. *Multidimensional Solid State NMR and Polymers*; Academic Press: London, 1994. (e) Ernst, R. R.; Bodenhausen, G.; Wokaun, A. *Principles of NMR in One and Two Dimensions*; Clarendon Press: Oxford, 1987.

(6) Buntkowsky, G.; Taupitz, M.; Roessler, E.; Vieth, H. M. *J. Phys. Chem. A* **1997**, *101*, 67.

(7) Nakai, T.; McDowell, C. A. *J. Am. Chem. Soc.* **1994**, *116*, 6373.

(8) (a) *Organikum*; VEB Verlag der Wissenschaften: Berlin, 1986. (b) Kling, B. Ph.D. Thesis, FU Berlin, 1996.

(9) (a) Brown, C. J. *Acta Crystallogr*. **1966**, *21*, 442. (b) Wasserman, H. J.; Ryan, R. R.; Layne, S. P. *Acta Crystallogr*. **1985**, *41*, 783.

(10) Spiess, H. W. *NMR Basic Principles and Progress*; Diehl, P., Fluck, E., Kosfeld, R., Eds.; Springer-Verlag: Berlin, 1978; Vol. 15, 58, pp 167−168.

(11) (a) Zabel, V.; Müller-Fahrnow, A.; Hilgenfeld, R.; Saenger, W.; Pfannemüller, B.; Enkelmann, V.; Welte, W. *Chem. Phys. Lipids* **1986**, *39*, 313. (b) Darbon-Meyssoniier, N.; Oddon, Y.; Decoster, E.; Pavia, A. A.; Pepe, G.; Reboul, J. P. *Acta Crystallogr*. **1985**, *C41*, 1324.

(12) Bennett, A. E.; Griffin, R. G.; Vega, S. *NMR Basic Principles and Progress*; Diehl, P., Fluck, E., Kosfeld, R., Eds.; Springer-Verlag: Berlin, 1994; Vol. 33, p 1.

(13) Hiyama, Y.; Niu, C. H.; Silverton, J. V.; Bavoso, A.; Torchia, D. A. *J. Am. Chem. Soc.* **1988**, *110*, 2378.